Delfim-Soares explicit time marching method for modelling of ultrasonic wave in microalgae pre-treatment

Delfim-Soares explicit time marching method for modelling of ultrasonic wave in microalgae pre-treatment

Wah Yen Tey[1,2,*], Kiat Moon Lee[3], Nor Azwadi Che Sidik[1] and Yutaka Asako[1]

1 Takasago i-Kohza, Malaysia-Japan International Institute of Technology, Universiti Teknologi Malaysia, Kuala Lumpur, Malaysia
2 Department of Mechanical Engineering, Faculty of Engineering, UCSI University, Kuala Lumpur, Malaysia
3 Department of Chemical and Petroleum Engineering, Faculty of Engineering, UCSI University, Kuala Lumpur, Malaysia
* Email of Corresponding Author: teywy@ucsiuniversity.edu.my

Abstract. Ultrasonic wave is one of the most popular pre-treatment methods of lipid extraction in microalgae, due to its low energy supply requirement, eco-friendliness and excellent cell disruption capability. Although quite some number of experimental works were reported, the numerical modelling of the ultrasonic wave in understanding the working principle of ultrasonic irradiation is limited so far, as to the knowledge of authors. The modelling is required for a more robust pre-treatment optimisation. Therefore, in current work, the numerical model of ultrasonic wave and its cavitation has been developed using the Delfim-Soares explicit time marching method (DSETM), which is proposed in recent years to solve structural vibration problem. The two dimensional wave equation in ultrasonic scale has been solved with the frequency of 20 kHz, 40 kHz and 60 Hz. Moreover, Rayleigh-Plesset equation is solved using the same method too to predict the growth of the radius of bubble due to different initial radius. It is found that higher wave frequency will not improve the speed of cavitation, but instead it can decrease the wavelength to increase the possibility of cavitation process occurrance in enhancing the pre-treatment efficiency.

1. Introduction

Microalgae are widely recognised with their high biomass production rate and energy efficiency among natural crops [1,2], and therefore they have been deemed as a promising source of renewable energy to substitute the fossil fuel [3]. The techniques of conversion of microalgae into biofuels can be found in many literatures [4–13] and proir to these biomass conversion, the extraction of lipids by breaking the lignin and hemicellulose structure is required [13,14]. In many conventional ways of lipids extraction (pre-treatment) such as mechanical milling [15], extrusion [16], acid/alkaline [17] and organosolv [18], high costing, environmental hazards and undesirable compounds formation appeared as their major disadvantages [13]. Ultrasonic irradiation is therefore one of the emerging pre-treatment technologies, which is eco-friendly and powerful in improving hydrolysis efficiency [19].

Ultrasonic wave is the acoustic wave with frequency ranging from 20 kHz and above, in which its compression and rarefactions will create acoustic bubbles. The bubbles will expand over time, and the void structure will implode as shock wave when critical bubble radius is developed. Such phenomenon is known as cavitation [20,21], and it will lead to temperature and pressure hike high enough to disrupt the lignocellulosic structure. The cavitation process can be illustrated in Figure 1. The point in which

the implosion occurs is named as *hotspot*. The details of the pre-treatment process due to ultrasonic wave can be further found in several archives [13,19–23].

Quite a number of works have been investigating on the production of biomass from different microalgae using ultrasonic method [24–28]. There are many other factors influencing the efficiency of ultrasonic pre-treatment such as biomass concentration, sonication intensity and power were reported [29–31]. However, most of the biomass investigations are limited to experimental works. The high cost and limited-variable range of experimental works will retard an in-depth study in microalgae pre-treatment. With this regards, the deployment of numerical mathematics for ultrasonic wave prediction could be an important alternative.

Nonetheless, the application of computational works in ultrasonic irradiation is in its infant stage. To the knowledge of authors, only Smithmaitrie and Tangudomkit [32] and Lais et al. [33] reported on the computational works in solving the fundamental ultrasonic equation with the assistance of finite element commercial software COMSOL. Moreover, the modelling of the ultrasonic cavitation is not available yet so far [33]. The very limited numerical works available in ultrasonic wave and cavitation have hindered further research on the computational prediction of pre-treatment efficiency and investigation on working principle of sonication. To fill the gap, Delfim-Soares explicit time marching (DSETM) Method will be applied in the current study. DSETM is proposed recently by Prof Delfrim Soares [34,35] to solve the structural mechanics problem, and now the method is being transplanted in current work to solve other hyperbolic equations in ultrasonic pre-treatment. Indeed, the method it is simpler to be implemented compared with conventional time discretisation as used by COMSOL for hyperbolic equation.

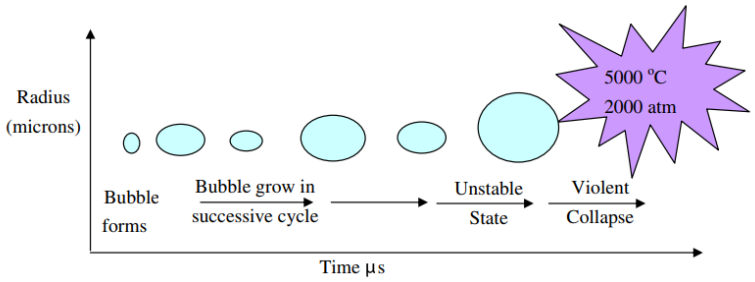

Figure 1. Cavitation process due to ultrasonic wave [21].

2. Mathematical modelling for ultrasonic wave equation

The modelling of two-dimensional ultrasonic wave is governed by the pressure acoustic equation which can be written as in Equation (1) [32,33,36]:

$$\frac{1}{\rho c^2}\frac{\partial^2 P_t}{\partial t^2}-\frac{1}{\rho}\left[\left(\frac{\partial^2 P_t}{\partial x^2}-\frac{\partial q_q}{\partial x}\right)+\left(\frac{\partial^2 P_t}{\partial y^2}-\frac{\partial q_q}{\partial y}\right)\right]=Q \tag{1}$$

where ρ is the fluid density [kg/m^3], c is the speed of sound [m/s], ρc^2 is the fluid bulk modulus [kg/(ms^2)], P_t is the total acoustic pressure [kg/(ms^2)], q_q is the dipole source [kg/(m^{2}s^2)], Q is the monopole source [1/s^2], t is time [s] while x and y represents the spatial coordinates [m]. Both monopole and dipole source are the directed acoustical sources [37], which influence the acoustic pressure at the far field as defined as in Equation (2) and (3) respectively:

$$P(r)=Q\frac{\rho c}{4\pi r\lambda} \tag{2}$$

$$P(r)=q_d\frac{\rho c d\cos\theta}{4\pi r\lambda^2} \tag{3}$$

in which r, λ, d and θ is the radius from the source of the acoustic vibration [m], wave length [m], distance between the acoustical sources [m] and angle between the acoustical sources respectively.

Equation (1) can be simplified into a simple wave equation by omitting the acoustical sources, as expressed in Equation (4).

$$\frac{\partial^2 P}{\partial t^2} = c^2\left(\frac{\partial^2 P}{\partial x^2} + \frac{\partial^2 P}{\partial y^2}\right) \tag{4}$$

The pressure compression and rarefaction will lead to acoustic cavitation and formation of bubbles. Therefore, upon numerical solution on Equation (1) or (4), the pressure field need to be corresponded with the bubble radius, which can be described by Rayleigh-Plesset equation [33,38] as in Equation (5):

$$\frac{P(t) - P_\infty(t)}{\rho} = R\frac{\partial^2 R}{\partial t^2} + \frac{3}{2}\left(\frac{\partial R}{\partial t}\right)^2 + \frac{4\nu}{R}\frac{\partial R}{\partial t} + \frac{2\sigma_s}{\rho R} \tag{5}$$

where P_∞, R, ν and σ_s represents the atmospheric pressure [kg/(ms^2)], bubble radius [m], kinematic viscosity of the fluid [m^2/s] and surface tension of the fluid [kg/s^2] respectively. The bubble radius will expand over time, and by reaching the critical radius, the bubble will collapse and release energy for cell wall disruption. Critical radius R_{cr} [39] can be expressed as in Equation (6):

$$R_{cr} = \sqrt{\frac{9mB_sT}{8\pi\sigma_s}} \tag{6}$$

where m, B_s and T is mass of gas in the bubble [kg], specific gas constant [J/(mol.K)] and absolute temperature [K] respectively. Equation (6) needs be modified into Equation (7), by assuming the geometry of the bubble as sphere:

$$R_{cr} = \sqrt{\frac{9B_sT}{8\pi\sigma_s}\left(\frac{4}{3}\pi R_{cr}^{\ 3}\right)} \leftrightarrow R_{cr} = \frac{2\sigma_s}{3\rho_a B_s T} \tag{7}$$

where ρ_a is the density of air [kg/m^3]. Upon explosion of bubble, the cavitation process will restart. By solving Equation (4) and (5), the contour of transient acoustic pressure and plot of bubble radius growth can be computed. The general numerical algorithm can be illustration in Figure 2.

However, the time required for the radius to reach its critical value is highly dependent on the initial radius [39]. Moreover, Rayleigh-Plesset equation is an initial value problem, but unfortunately there is no mathematical equation available to predict the initialisation of bubble formation. In the work of Chakma and Moholkar [40], the initial radius is prescribed instead of computed. The assumption on the initial radius is required prior to computation.

3. Physical Modelling

In current work, the ultrasonic transducer is located at the middle of the microalgae-fluid domain. The microalgae-fluid domain is set in square shape with area of 0.04 m^2 (20 cm × 20 cm), while the size of the transducer is at the middle of the domain, as shown in Figure 3. The ultrasonic transducer is supplied with the frequency f of 20 kHz, 40 kHz and 60 kHz. The implementation of the boundary conditions will be further discussed in the next section. Meanwhile the fluid domain properties applied can be summarised in Table 1.

Table 1. Applied fluid domain properties.

Fluid Properties	Value (Unit)
Absolute temperature T	300 K
Density of microalgae-fluid ρ	1000 kg/m^3
Kinematic viscosity of microalgae-fluid ν	9×10^{-5} m^2/s
Surface tension of microalgae-fluid σ_s	7×10^{-2} kg/s^2
Density of air ρ_a	1 kg/m^3
Specific gas constant B_s	8.314 J/(mol.K)

Based on the properties set above, the critical radius R_{cr} is therefore 1.871×10^{-5} m or 18.71 μm, according to Equation (7). As soon as the bubble radius develops as big as 18.71 μm, Equation (5) needs to be solved again.

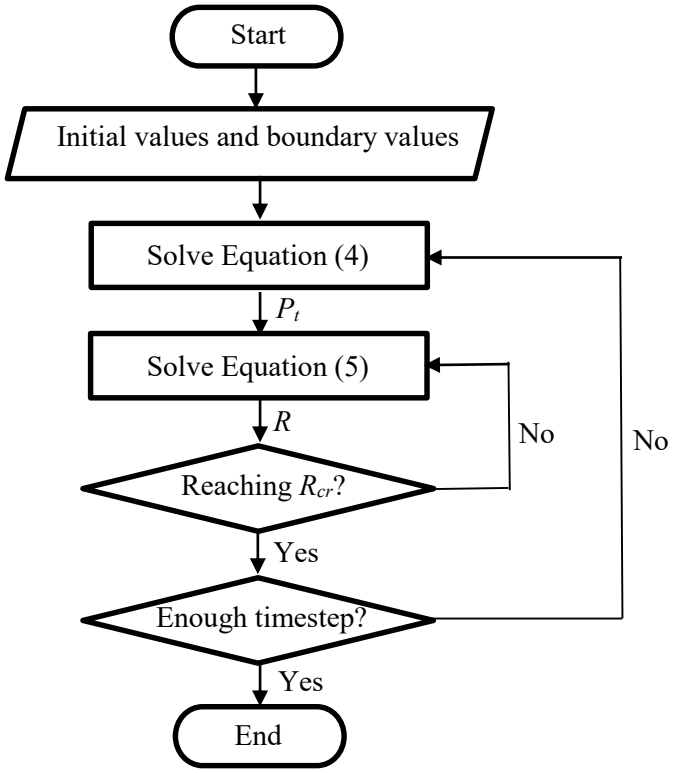

Figure 2. Numerical algorithm for computation of ultrasonic wave and cavitation.

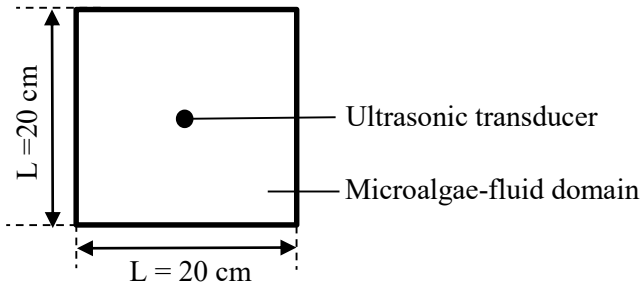

Figure 3. Physical modelling of problem domain.

4. Numerical Modelling

Time marching scheme for hyperbolic equation plays an important role in computational physics as the acceleration term always lead to numerical instability. Most of the time marching scheme applied is the central differencing time marching (CDTM), but the scheme requires three storage of memory in every iteration, i.e. the previous, current and future field variables. There are works [41,42] which applied the higher order time marching scheme, nonetheless, this will aggravate the complexity in the initialisation of computation. The complete review can be found also in the work of Tamma et al. [43].

To mitigate the issue, Soares proposed a novel explicit time marching scheme, [34,35], in which the current field variable is the only criteria to initial the hyperbolic computation. The method is simple to execute. Time integration of Equation (4) is:

$$\int_{\Delta t}^{t+\Delta t} \frac{\partial^2 P}{\partial t^2} dt = c^2 \int_{t}^{t+\Delta t} \frac{\partial^2 P}{\partial x^2} dt + c^2 \int_{t}^{t+\Delta t} \frac{\partial^2 P}{\partial y^2} dt$$

which will lead to

$$\left(\frac{\partial P}{\partial t}\right)^{n+1} = \left(\frac{\partial P}{\partial t}\right)^{n} + \frac{c^2 \Delta t}{\Delta x^2}\left(P_{i+1,j}{}^{n} + P_{i-1,j}{}^{n} + P_{i,j+1}{}^{n} + P_{i,j-1}{}^{n} - 4P_{i,j}{}^{n}\right) \tag{8}$$

$$P_{i,j}{}^{n+1} = P_{i,j}{}^{n} + \left(\beta_1 \left(\frac{\partial P}{\partial t}\right)_{i,j}^{n} + \beta_2 \left(\frac{\partial P}{\partial t}\right)_{i,j}^{n+1}\right)\Delta t \tag{9}$$

where Δx, Δt and n is the node spatial distance, field variable time marching interval and current time step respectively, while β_1 and β_2 are time marching coefficients [35]. The only variable needed to initiate the computation is the wave excitation at the middle of the domain, which can be described as:

$$P_{I,J} = P_{\max} \sin\left(2\pi f t\right) \tag{10}$$

where (I,J) is the location of wave excitation while $P_{\max}$ is the amplitude of acoustic pressure. Since the ultrasonic wave emits about 10 dB of sound pressure level, the corresponding $P_{\max}$ is 3.1623 μPa. The non-reflecting boundary condition is applied.

Now the DSETM approximation of Equation (5) is:

$$\left(\frac{\partial R}{\partial t}\right)^{n+1} = \left(\frac{\partial R}{\partial t}\right)^{n} - \left(R^n\right)^2 \left[1.5\left(R^n\right)\left[\left(\frac{\partial R}{\partial t}\right)^{n}\right]^2 + 4\nu\left(\frac{\partial R}{\partial t}\right)^{n} + \frac{2\sigma_s + \left(R^n\right)\left(P_\infty(t) - P_t(t)\right)}{\rho}\right] = 0 \tag{11}$$

$$R^{n+1} = R^n + \Delta t \left(\frac{\partial R}{\partial t}\right)^{n+1} \tag{12}$$

During the computation of Equation (4) and (5), the Courant Number C as defined in Equation (13), must be controlled within 1 to ensure numerical stability during time marching. In the current work, the Courant number applied is 0.5 to ensure the fulfilment of Courant-Friedrichs-Lewy (CFL) condition [44,45].

$$C = \frac{c\Delta t}{\Delta x} \leftrightarrow \Delta t = 0.5\frac{\Delta x}{c} \tag{13}$$

Note that the time step shall be sufficient to support the ultrasonic frequency, i.e. $\Delta t < 1/f$. Anyhow, Eq. (13) is ample to ensure time-marching stability indeed as $0.5\Delta x/c^2$ is always larger then $1/f$. Meanwhile for the simulation on Rayleigh-Plesset equation is conducted with initial radius of 1.8, 2.5, 3.4, 4.2 and 5.0 μm [40].

5. Numerical Verification

The numerical verification is done by comparing the results obtained for one-dimensional wave equation using DSETM and CDTM. By setting the initial and boundary conditions as described in Section 4, both DSETM and CDTM will produce the similar sinusoid curve as shown in Figure 4. Moreover, the wavelength of the wave is in accordance with the established relationship [46] between the wavelength, frequency and speed of sound, i.e. for frequency of 20 Hz, the wave length, λ is:

$$c = f\lambda \leftrightarrow \lambda = \frac{c}{f} = 0.0172\text{m} = 0.172 \times 10^5\ \mu\text{m} \tag{14}$$

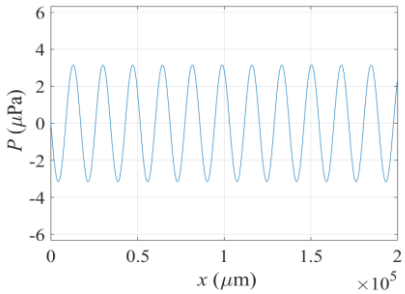

Figure 4. Sinusoid curve produced by DSETM and CDTM for one-dimensional wave equation.

6. Results and Discussion

There are three possible ways in which the ultrasonic wave improves the pre-treatment: the initiation of cavitation, initial radius of acoustic bubble and its growth rate. The effect of wave frequency to these factors will be investigated.

The effect of frequency to initiation of cavitation can be studied via the modelling of ultrasonic wave produced by the excitation with different frequencies. Transducer frequency of 20 kHz, 40 kHz and 60 kHz within the time of 500 μs can be observed as in Figures 5 – 7 respectively. The higher the frequency, the smaller the wavelength. With the reduction of wavelength, acoustic pressure fluctuates at almost every location of domain within the same time frame. This will increase the possibility to implode the cavitation bubbles as the implosion is a direct outcome of pressure compression [47].

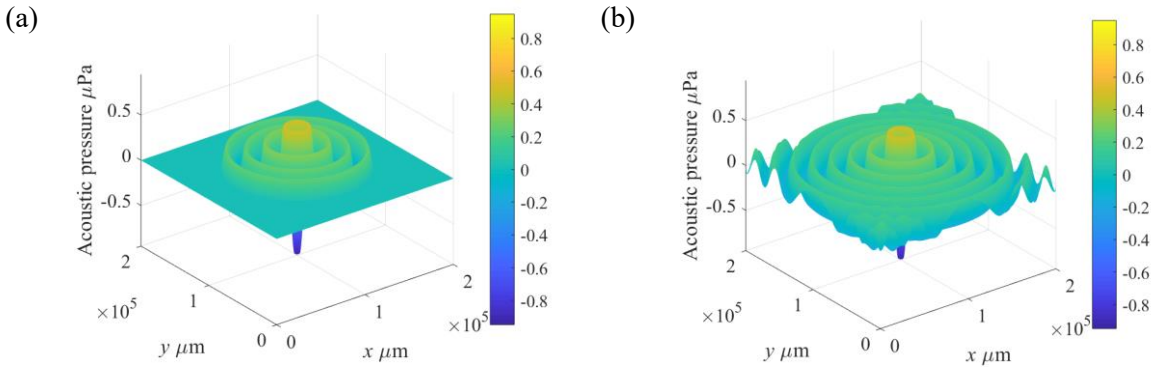

Figure 5. Development of ultrasonic wave of 20 kHz at the time of (a) 200 μs and (b) 500 μs.

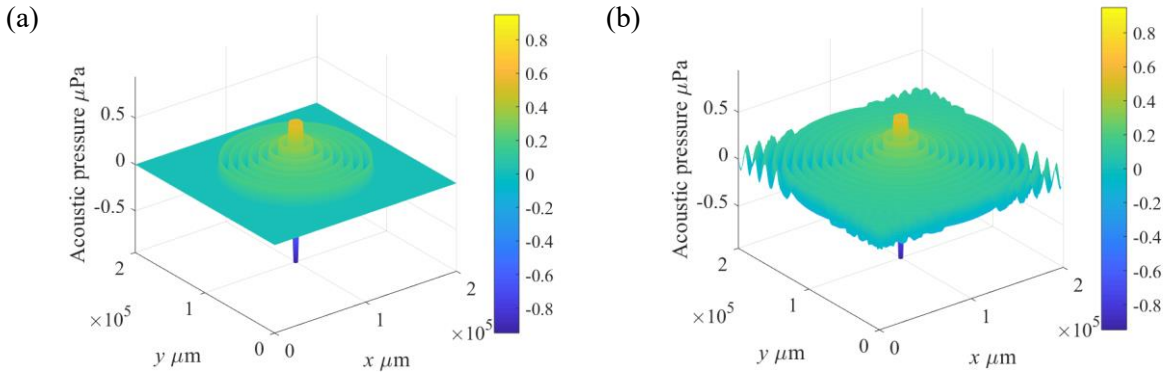

Figure 6. Development of ultrasonic wave of 40 kHz at the time of (a) 200 μs and (b) 500 μs.

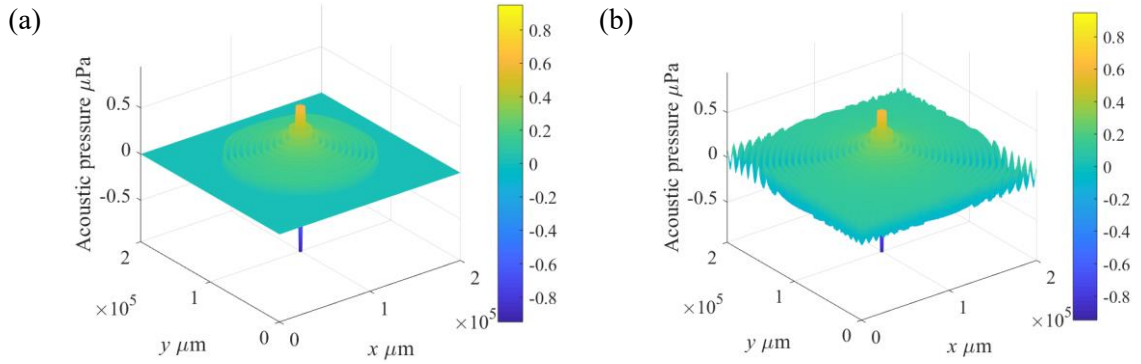

Figure 7. Development of ultrasonic wave of 60 kHz at the time of (a) 200 μs and (b) 500 μs.

The growth of radius of the cativation bubble due to different initial radius has also been computed in Figure 8. The time required for bubble collapse increases with the radius of initial bubble formed. It can be observed that during the radius expansion, there are two patterns along the way: (a) the radius grows exponentially with time in general; (b) the radius expands and shrinks alternatively during the general exponential growth due to the pressure fluctuation. It can be clearly shown that the larger initial bubble will shorten the time for implosion. However, the formation of initial radius somehow is beyond the control of experiments [47]. Figure 8 can complement the unknown curve of radius expansion as in Figure 1.

The successful implementation of the DSETM Method to solve the wave equation lays a cornerstone for future manipulation of more variables to model the ultrasonic wave. This may include the effects of increment of pressure amplitude, interference modelling (coherent or non-coherent source) and various possible wall boundary condition and geometry.

However, the frequency does not influence the speed of growth of the bubble radius as shown in Table 2. The growth of radius is more dependent on other fluid properties. Ultrasonic wave is just a sparking factor to initiate the acoustic cavitation. However, it is noteworthy that frequency plays it role in such a way that: the higher frequency will enable more “dormant” bubbles to be geared towards implosion and energy release.

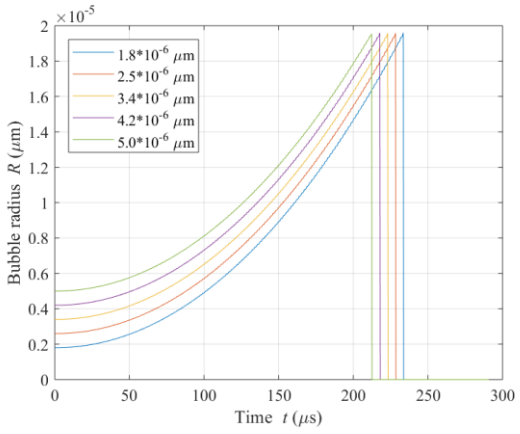

Figure 8. The computation radius expansion using DSETM at different initial bubble radius.

Table 2: Implosion time required for acoustic bubble with initial radius of 5 μm.

Frequency (kHz)	Time required for implosion (μs)
20	233.7228
40	233.7228
60	233.7228

7. Conclusion

In conclusion, DSETM scheme has been extended from structural mechanics for application in computation of ultrasonic wave and acoustic cavitation. It is found that the high frequency does not increase the speed of growth of acoustic bubbles, but it does enhance the possibility for the initialisation of cavitation process. This study has paved a computational basis for a more complex modelling in ultrasonic wave and cavitation. Nevertheless, the computational works is unable to predict the hotspot formation and location, due to the lack of mathematical description on the spatial information of acoustic cavitation occurance. This could be a potential area for further investigation as well.

Acknowledgment

The authors who like to thank the support from the Takasago Research Fund, channelled by Takasago International Corporation, Japan. This research is also partially supported by Pioneer Scientist Incentive Fund (PSIF) with grant number Proj-In-FETBE-038, Centre of Excellence for Research, Value Innovation and Entrepreneurship (CERVIE), UCSI University Kuala Lumpur, Malaysia.

References

[1] Zheng H, Yin J, Gao Z, Huang H, Ji X and Dou C 2011 Disruption of Chlorella vulgaris cells for the release of biodiesel-producing lipids: A comparison of grinding, ultrasonication, bead milling, enzymatic lysis, and microwaves *Appl. Biochem. Biotechnol.* **164** 1215–24

[2] Bomgardner M M 2012 Flying the green skies with biofuels: with test flights behind them, airlines push for more production of biobased jet fuel *Chem. Eng. News* 18–21

[3] Rupprecht J 2009 From systems biology to fuel-Chlamydomonas reinhardtii as a model for a systems biology approach to improve biohydrogen production *J. Biotechnol.* **142** 10–20

[4] Bhatt N C, Panwar A, Bisht T S and Tamta S 2014 Coupling of algal biofuel production with wastewater *Sci. World J.* Article ID 210504

[5] Jegathese S J P and Farid M 2014 Microalgae as a renewable source of energy: A niche opportunity *J. Renew. Energy* Article ID 430203

[6] Chen W H, Lin B J, Huang M Y and Chang J S 2015 Thermochemical conversion of microalgal biomass into biofuels: A review *Bioresour. Technol.* **184** 314–27

[7] Yu I K M and Tsang D C W 2017 Conversion of biomass to hydroxymethylfurfural: A review of catalytic systems and underlying mechanisms *Bioresour. Technol.* **238** 716–32

[8] Dhyani V and Bhaskar T 2017 A comprehensive review on the pyrolysis of lignocellulosic biomass *Renew. Energy* **129** 695–716

[9] Adams P, Bridgwater T, Lea-Langton A, Ross A and WatsonI 2018 Chapter 8 - Biomass Conversion Technologies *Greenhouse Gas Balances of Bioenergy Systems* pp 107–39

[10] Widjayaa E R, Chena G, Bowtella L and Hills C 2018 Gasification of non-woody biomass: A literature review *Renew. Sustain. Energy Rev.* **89** 184–93

[11] Wirth R, Lakatos G, Böjti T, Maróti G, Bagi Z, Rákhely G and Kovács K L 2018 Anaerobic gaseous biofuel production using microalgal biomass – A review *Anaerobe* **52** 1–8

[12] Luo Y, Li Z, Li X, Liu X, Fan J, Clark J H and Hu C 2018 The production of furfural directly from hemicellulose in lignocellulosic biomass: A review *Catal. Today* In Press, Corrected Proof

[13] Hassan S S, Williams G A and Jaiswal A K 2018 Emerging technologies for the pretreatment of lignocellulosic biomass *Bioresour. Technol.* **262** 310–8

[14] Sun S, Sun S, Cao X and Sun R 2016 The role of pretreatment in improving the enzymatic

hydrolysis of lignocellulosic materials *Bioresour. Technol.* **199** 49–58
[15] Rodriguez C, Alaswad A, El-Hassan Z and Olabi A G 2017 Mechanical pretreatment of waste paper for biogas production *Waste Manag.* **68** 157–64
[16] Duque A, Manzanares P and Ballesteros M 2017 Extrusion as a pretreatment for lignocellulosic biomass: Fundamentals and applications *Renew. Energy* **114** 1427–41
[17] Shimizu F L, Monteiro P Q, Ghiraldi P H C, Melati R B, Pagnocca F C, Souza W, Sant'Anna C and Brienzo M 2018 Acid, alkali and peroxide pretreatments increase the cellulose accessibility and glucose yield of banana pseudostem *Ind. Crops Prod.* **115** 62–8
[18] Salapa I, Katsimpouras C, Topakas E and Sidiras D 2017 Organosolv pretreatment of wheat straw for efficient ethanol production using various solvents *Biomass and Bioenergy* **100** 10–6
[19] Karimi M, Jenkis B and Stroeve P 2014 Ultrasound irradiation in the production of ethanol from biomass *Renew. Sustain. Energy Rev.* **40** 400–21
[20] Le N T, Julcour-Lebigue C and Delmas H 2015 An executive review of sludge pretreatment by sonication *J. Environ. Sci.* **37** 139–53
[21] Pilli S, Bhunia P, Yan S, LeBlanc R J, Tyagi R D and Y S R 2011 Ultrasonic pretreatment of sludge: a review *Ultrason. Sonochem.* **18** 1–18
[22] Luo J, Fang Z and Smith Jr R L 2014 Ultrasound-enhanced conversion of biomass to biofuels *Prog. Energy Combust. Sci.* **41** 56–93
[23] Sivaramakrishnan R and Incharoensakdi A 2018 Microalgae as feedstock for biodiesel production under ultrasound treatment - A review *Bioresour. Technol.* **250** 877–87
[24] Surendhiran D and Vijay M 2014 Effect of various pretreatment for extracting intracellular lipid from nannochloropsis oculata under nitrogen replete and depleted conditions *ISRN Chem. Eng.* Article ID 536310
[25] Kwangdinata R, Raya I and Zakir M 2014 Production of biodiesel from lipid of phytoplankton Chaetoceros calcitrans through ultrasonic method *Sci. World J.* Article ID 231361
[26] Nogueira D A, da Silveira J M, Vidal E M, Ribeiro N T and Burkert 2018 Cell disruption of Chaetoceros calcitrans by microwave and ultrasound in lipid extraction *Int. J. Chem. Eng.* Article ID 9508723
[27] Juttuporn W, Thiengkaew P, Rodklongtan A, Rodprapakorn M and Chitprasert P 2018 Ultrasound-assisted extraction of antioxidant and antibacterial phenolic compounds from steam-exploded Sugarcane Bagasse *Sugar Tech* **20** 599–608
[28] Guo P, Zheng C, Huang F, Zheng M, Deng Q and Li W 2013 Ultrasonic pretreatment for lipase-catalyzed synthesis of 4-methoxy cinnamoyl glycerol *J. Mol. Catal. B Enzym.* **93** 73–8
[29] Zou S, Wang X, Chen Y, Wan H and Feng Y 2016 Enhancement of biogas production in anaerobic co-digestion by ultrasonic pretreatment *Energy Convers. Manag.* **112** 226–35
[30] Babaei Z, Chermahini A N, Dinari M, Saraji M and Shahvar A 2018 Cleaner production of 5-hydroxymethylfurfural from fructose using ultrasonic propagation *J. Clean. Prod.* **198** 381–8
[31] de Farias Silva C E, Meneghello D, de Souza Abud A K and Bertucco A 2018 Pretreatment of microalgal biomass to improve the enzymatic hydrolysis of carbohydrates by ultrasonication: yield vs energy consumption *J. King Saud Univ. - Sci.* In Press, Accepted Manuscript
[32] Smithmaitrie P and Tangudomkit K 2018 Multiphysics finite element modeling and validation of transient aerosol generation in an ultrasonic nebulizer drug delivery device *J. Aerosol Sci.* **216** 110–21
[33] Lais H, Lowe P S, Gan T H and Wrobel L C 2018 Numerical modelling of acoustic pressure fields to optimize the ultrasonic cleaning technique for cylinders *Ultrason. - Sonochemistry* **45** 7–16
[34] Soares D 2016 A novel family of explicit time marching techniques for structural dynamics and wave propagation models *Comput. Methods Appl. Mech. Eng.* **311** 838–55
[35] Soares D 2015 A simple and effective new family of time marching procedures for dynamics *Comput. Methods Appl. Mech. Eng.* **283** 1138–66
[36] COMSOL 2008 *Acoustic Module Model Library*

[37] Russell D A, Titlow J P and Bemmen Y-J 1999 Acoustic monopoles, dipoles, and quadrupoles: An experiment revisited *Am. J. Phys.* **67** 10.1119/1.19349
[38] Plesset M S and Prosperetti A 1977 Bubble dynamics and cavitation *Annu. Rev. Fluid Mech.* **9** 145–85
[39] Morch K A 2009 Cavitation nuclei: Experiments and theory *J. Hydrodyn.* **21** 176–89
[40] Chakma S and Moholkar V S 2013 Numerical simulation and investigation of system parameters of sonochemical process *Chinese J. Eng.* Article ID 362682
[41] Soroushian A and Farjoodi J 2008 A unified starting procedure for the Houbolt method *Commun. Numer. Methods Eng.* **24** 1–13
[42] Young D L, Gu M H and Fan C M 2009 The time-marching method of fundamental solutions for wave equations *Eng. Anal. Bound. Elem.* **33** 1411–25
[43] Tamma K K, Zhou X and Sha D 2000 The time dimension: A theory towards the evolution, classification, characterization and design of computational algorithms for transient/ dynamic applications *Arch. Comput. Methods Eng.* **7** 67–290
[44] Kajishima T and Taira K 2017 *Computational Fluid Dynamics: Incompressible Turbulent Flows* (Springer International Publishing)
[45] Gnedin N Y, Semenov V A and Kravtsov A V 2018 Enforcing the Courant-Friedrichs-Lewy condition in explicitly conservative local time stepping schemes *J. Comput. Phys.*
[46] Kinsler L E, Frey A R, Coppens A B and Sanders J V 2000 *Fundamentals of Acoustics* (John Wiley & Sons, Inc)
[47] Tyagi K, Lo S L, Appels L and Dewil R 2014 Ultrasonic treatment of waste sludge: A review on mechanisms and applications *Crit. Rev. Environ. Sci. Technol.* **1120**–**1288** 2014